Thermodynamic Mechanism of Free Heme Action on Sickle Cell Hemoglobin Polymerization

Anupam Aich, Weichun Pan, and Peter G. Vekilov
Department of Chemical and Biomolecular Engineering, University of Houston, Houston, TX 77204

DOI 10.1002/aic.14800
Published online April 8, 2015 in Wiley Online Library (wileyonlinelibrary.com)

For insights into the mechanisms of heme action on the rate of sickle cell hemoglobin polymerization, we determine the erythrocytic concentration of free heme using a novel method based on enzymatic catalysis and luminescence. We find in sickle cell patients 44 ± 10 μM, in sickle trait individuals, 33 ± 4 μM, and in healthy adults, 21 ± 2 μM. We test the applicability of two mechanisms of heme action: a kinetic one, whereby heme aggregates serve as heterogeneous nucleation centers, and a thermodynamic pathway, in which free heme enhances the attraction between sickle hemoglobin (HbS) molecules in solution. We show that the latter mechanism exclusively operates. The enhanced attraction leads to increase of the total volume of a population of dense liquid clusters by about two orders of magnitude. As the dense liquid clusters serve as locations and precursors to the formation of the HbS polymer nuclei, their increased volume directly leads to faster polymer nucleation. © 2015 American Institute of Chemical Engineers *AIChE J*, 61: 2861–2870, 2015

Keywords: sickle hemoglobin, free heme, heterogeneous nucleation, two-step nucleation, intermolecular interactions

Introduction

Sickle-cell anemia was the first disease whose molecular basis was identified: in 1949 Pauling's group used one of the first capillary electrophoresis devices and showed that hemoglobin from sickle cell patients had excess of positive charge in comparison with hemoglobin from healthy adults.[1,2] The sequences of sickle (HbS) and normal adult (HbA) hemoglobins showed that the charge difference detected by Pauling and his coworkers was due to a mutation from glutamate to valine at the sixth site of the two β-chains of hemoglobin.[3] Further studies showed that HbS forms 14-member fibers[4–6] when the protein is in its T-conformation[7] in the deoxy-state. The crucial role of the mutation to valine is that in the fibers, hydrophobic contacts are formed between valine of one HbS molecule and alanine, phenylalanine, and leucine from an adjacent HbS molecule.[5,6,8,9] The fibers were shown to stretch and deform the red blood cells,[10] and dramatically alter their mechanical and rheological properties.[11,12] The modified red blood cells pass more slowly than normal cells through the venous circulation.[13] In combination with several processes involving the endothelial walls and the other blood components, leucocytes, platelets, and so forth, erythrocyte sickling frequently leads to vasoocclusion. The associated damage of the affected organs, pain, and often death are the main clinical manifestations of sickle cell anemia.[14]

Heme, Fe^{2+} propoporphirin IX, is the main prosthetic group of both sickle and normal hemoglobin. Each hemoglobin molecule carries four hemes, one per each of its subchains. One or more (less likely) of the hemoglobin hemes may be released to the solution,[15,16] Figure 1a. The release occurs predominantly after its autoxidation to methemoglobin, in which the iron is in its Fe^{3+} form.[16,17] Hence, the heme released from hemoglobin is in the form of hematin, that is, Fe^{3+} protoporphyrin IX with an OH^- ligand. The stability of HbS to autoxidation is lower than that of normal adult HbA.[17] Heme is a substance with proven toxicity, which triggers lyses of human erythrocytes[18] and other cell types.[19,20] It has been suggested that the release of heme may cause higher severity and frequency of sickle cell crises by binding to the red cell membrane leading to membrane damage[21] and stronger adhesion of sickle red cells to leucocytes and the endothelium.[22–24]

The sequence of events leading from the sickle cell mutation and HbS expression through polymerization to vasoocclusion and pain crisis is well understood and has classified the disease as a monogenically inherited disorder. In a strong deviation from trends typical of such conditions, sickle cell exhibits significant clinical heterogeneity[25] and extreme variability even among patients with identical genotypes.[26] This heterogeneity and variability have been attributed to polymerization-independent mechanisms such as red cell membrane damage and enhanced adhesivity, endothelial activation, lymphocyte and platelet aggregation, and others.[27,28] Recently, we provided evidence of the action of a novel factor for the variability of sickle cell disease: we showed that in the presence of free heme, the rate of HbS polymerization accelerates by up to two orders of magnitude.[29]

Besides providing novel fundamental understanding into the physiological pathways of sickle cell disease, the finding of the role played by free intraerythrocytic heme could potentially open novel avenues for the treatment of sickle cell.

Correspondence concerning this article should be addressed to P. G. Vekilov at vekilov@uh.edu

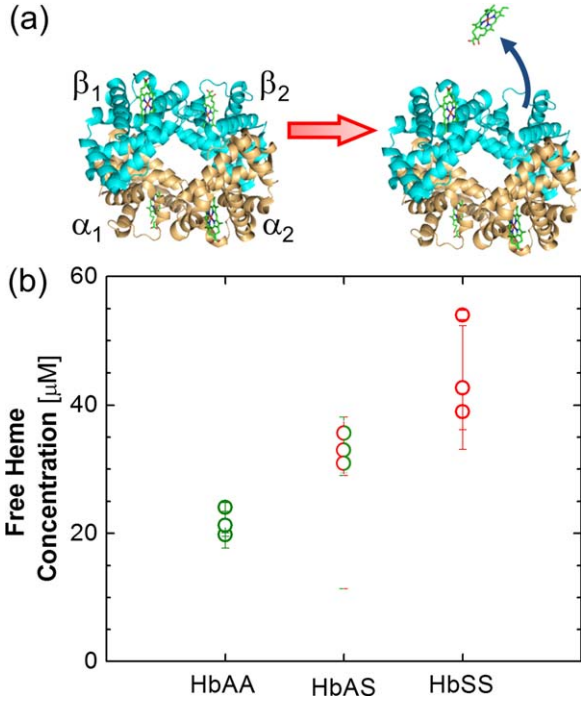

Figure 1. The release of heme.

(a) Schematic of heme release from met-hemoglobin. α- and β-chains of hemoglobin are drawn in brown and blue, respectively; the C-atoms of heme, in green. Heme is predominately released form the β-chains. (b) The average concentrations of free heme in blood samples of thee sickle cell patients, three sickle trait individuals, and three healthy donors. Six donations of four 4 mL tubes were obtained from healthy donor 1 and two from healthy donor 2 and are averaged; all other data points are averages over four tubes of one donation. [Color figure can be viewed in the online issue, which is available at wileyonlinelibrary.com.]

These avenues could entail, for instance, suppressing heme release from hemoglobin or enhancing the metabolic pathways of heme degradation.[29] However, before free heme can become a viable target for sickle cell therapies, several questions about its action need to be addressed. Among them are:

1. What is the concentration of free heme in sickle erythrocytes? A single previous determination of the concentration of free heme in sickle and healthy erythrocytes[30] found concentrations of, respectively, 0.75 and 0.15 μM. These concentration are lower by about two orders of magnitude than those tested for their effects on HbS polymerization and would preclude any effects of free heme on polymerization.[29]
2. What is the mechanism of action of free heme on polymerization? Free heme may accelerate polymerization by at least two distinct mechanisms. In aqueous solutions hematin has a proven propensity to aggregate[31,32] and the incipient aggregates may serve as heterogeneous nucleation centers; foreign substrates are known to enhance the rates of nucleation of condensed phases by orders of magnitude.[33] An alternative mechanism of heme action involves enhanced attraction between hemoglobin molecules in solution. Much fewer details about this potential pathway of heme action on the kinetics of HbS polymerization are understood even in principle.

The goal of the investigations presented here is to elucidate these two questions. It gives us great pleasure to publish these results in a tribute to Professor John Prausnitz. John has proposed, implemented, and advocated the application of thermodynamic methods and insights to problems of ever increasing complexity, including those of biomedical origins.[34,35] He might appreciate our main conclusion that the mechanism selected by free heme to enhance HbS polymerization is thermodynamic: free heme enhances the intermolecular attraction in the solution and in this way stabilizes a dense liquid cluster phase that serves as an essential precursor for the nucleation of HbS fibers. The stabilized cluster phase occupies a total volume higher by two orders of magnitude and this allows for correspondingly faster nucleation.

Experimental Procedures

Determination of free heme

The overwhelming difficulty in the determination of free heme in erythrocytes is its separation from hemoglobin without additional heme release or loss of existing free heme; even advanced spectroscopy methods fail to quantify free heme in the presence of hemoglobin.[36] Most of the recent work on heme quantification has focused on the determination of the total heme content, including the one bound to globins, often in the context of forensics.[37] Earlier methods were mostly based on the spectroscopic response of heme and heme-containing proteins[38]; recent studies rely on HPLC,[39] capillary electrophoresis[40] and other electrochemical methods,[41] and, most recently, mass spectrometry.[37,42]

We developed a new, sensitive and selective, method of heme quantification based on quantitative reconstitution of apo-horse radish peroxidase (apo-HPR) in the presence of heme,[43] followed by determination of the rate of the peroxidase reaction using luminescence detection. We use blood from sickle, sickle trait (i.e., heterozygous for sickle and normal hemoglobins), and healthy donors, drawn according to institutional regulations, and isolate the erythrocytes. We then lyse them in water and separate the released hematin from hemoglobin and other high molecular weight erythrocyte components by dialysis of the hemolysate at ~5°C. The resulting hematin concentration in the dialysate is less than 1 nM. To efficiently quantify such low concentrations, we combine the enzymatic action of reconstituted horse radish peroxidase with luminescence monitoring of the rate of the peroxidase reaction. The sequence of reactions that underlie the method is

$$\text{Apo-HRP} + \text{Heme} \rightarrow \text{HRP} \tag{1a}$$

$$\text{HRP} + \text{H}_2\text{O}_2 \rightarrow \text{HRP} + 2\ \text{HO}\cdot \tag{1b}$$

$$\text{HO}\cdot + \text{luminol} \rightarrow \text{Aminophthalate} + h\nu \tag{1c}$$

Reaction (1c) is accompanied by luminescence at 428 nm.[44,45] The luminescence intensity is proportional to the rate of catalytic decomposition of peroxide. This rate, in turn, is proportional to the concentration of reconstituted peroxidase. In excess of apo-HRP, the concentration of the reconstituted enzyme equals that of the initial heme. Hence, the luminescence intensity is proportional to the concentration of free heme. The transformation of the analyte to a catalyst of a reaction with a well detectable product underlies the high sensitivity of this method. Furthermore, the luminol reaction is an example of very strong chemiluminescence.[44,45] The strong amplification of the signal allows detection and quantification of hematin levels as low as 50 pM.

We showed that the method is robust and accurate within ± 5%. We demonstrated that additional heme is not released during storage of blood and hemolysate at ~5°C, two steps in the experimental procedure. We showed that no new heme is released in the hemolysate during dialyses. Additional tests revealed that the found heme is not released from the erythrocyte membranes. Thus, the hematin found in the dialysate comes exclusively from the erythrocyte cytosol. Furthermore, we do not expect any heme loss due to, for example, crystallization or other aggregation: during all analysis steps after the red cell lysis, the concentration of free heme is kept low, below 500 nM.

Characterization of aggregation of heme, HbS clusters, and interactions between hemoglobin molecules

The formation of hematin aggregates and dense liquid clusters in deoxy-HbS solutions, held in sealed cuvettes, was characterized by dynamic light scattering[46]; interactions between deoxy-HbS molecules in solution and their modifications by free heme were characterized by static light scattering.[47,48] Both methods used a ALV-5000/EPP static and dynamic light scattering device (ALV-Gmbh, Langen, Germany) with a 35 mW He-Ne laser operating at wavelength λ= 632.8 nm (Uniphase), for further experimental details, see Refs. 46,47.

The Intraerythrocytic Concentration of Free Heme

We determined the average concentrations of free heme in the erythrocytes of three sickle cell patients and equal numbers of sickle trait and healthy donors. From the results in Figure 1b, the average of sickle cell patients is 44 ± 10 μM, sickle trait donors, 33 ± 4 μM, and healthy donors, 21 ± 2 μM. The variation between individual donors is significantly higher for sickle cell patients than for healthy and sickle trait donors.

The results in Figure 1b for both sickle and normal hemoglobin are about two orders of magnitude higher than the previous determination of Liu et al.[30] Liu et al. separated free heme from hemoglobin by charge, using ion exchange liquid chromatography,[30] in contrast to the separation by size using dialyses, used by us. To isolate the hematin, Liu et al. added 2 M NaCl to the hemolysates. At this electrolyte concentration, they assumed that hematin would be retained on the chromatography column, to be eluted by a solution of sodium dodecyl sulfate (SDS) for subsequent quantification. To validate the method, Liu et al. added hematin to the hemolysate and retrieved 75% of the added amount after the SDS elution. Experiments, reveal that the addition of 2 M NaCl has different consequences for free heme stoichiometric to apoglobin and that in excess of the stoichiometric ratio. In the latter case, we showed that hematin is precipitated. We conclude that the hematin added for calibration by Liu et al. was precipitated, retained as a solid at the top of the column and subsequently dissolved and eluted by SDS for nearly complete recovery. Conversely, hematin in stoichiometric ratio to apoglobin was driven back to the apoglobin due to its high chemical potential in the presence of NaCl. Hence, it is not separated from the hemoglobin on passage through the chromatography column. This explain the low free heme concentrations detected by Liu et al.[30]

The concentrations of free heme in sickle erythrocytes in Figure 1b are comparable to those that induce ca. 100× acceleration of the nucleation of sickle cell polymers.[29]

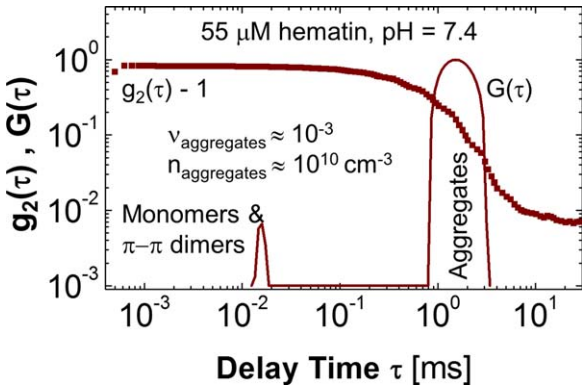

Figure 2. Characterization of the aggregation state of a hematin solution of indicated concentration by dynamic light scattering.

Both the correlation function $g_2(t)$ and the intensity distribution function $G(t)$ are shown. [Color figure can be viewed in the online issue, which is available at wileyonlinelibrary.com.]

Thus, free intraerythrocytic heme may be a powerful factor that enhances the rate of polarization. The mechanism of this enhancement is discussed below.

Does Heme Provide Heterogeneous Centers for HbS Polymer Nucleation?

Nucleation assisted by foreign substrates that interacts favorably with the new phase was first discussed by Gibbs.[49–51] The accepted role of the foreign substrate is to lower the free energy barrier that determines the nucleation rate. The recent focus in the area has been on the structural and chemical correspondences between the nucleating phase and the substrate.[52–56] In aqueous solutions hematin may polymerize into loosely bound large linear aggregates[32] that may serve as heterogeneous nucleation centers.

To judge the presence of hematin oligomers and larger amorphous aggregates, we performed a dynamic light scattering characterization of a 55 μM solution of hematin at pH = 7.4 in 0.15 M phosphate buffer. This buffer is considered an adequate model of the red cell cytosol; the hematin concentration is representative of the value for sickle erythrocytes in Figure 1b. To imitate the slow release of heme in the erythrocytes, the solution was prepared by dissolving dry powder in 0.1 M NaOH at pH = 13 to a concentration of ~2 mM, below its solubility at this pH.[57] We then slowly lowered the solution pH to 7.4 by addition of H_3PO_4 and/or KH_2PO_4. Characterization of the aggregation state of this solution by dynamic light scattering in Figure 2 reveals the presence of small scatterers diffusing with characteristic time τ_1 from 13 to 16 μs and larger entities diffusing with $\tau_2 \approx 1$ ms. The time τ_1 indicates that the small scatterers are a mixture of monomers and π–π dimers.[32] The relatively high dimerization constant[31] indicates that in this mixture the dimers are ca. 99%. The large entities with τ_2 have radius of ~80 nm and are likely hematin aggregates; in view of the known slow crystallization of hematin in aqueous solutions,[58,59] they are likely amorphous.

To evaluate the fraction of hematin occluded in the aggregates, we compare the total intensity scattered by the aggregates to that scattered by the monomers and dimers. We evaluate the ratio of the intensities scattered by the 80 nm aggregates and the monomers from the ratio of the areas of

the respective peaks A_2/A_1 in Figure 2, 600:1. The fraction of hematin in the aggregates $v_{aggregates}$ is approximately equal to the ratio of the volume fractions of the aggregates and monomers, A_2/A_1.[60] Assuming that aggregates exhibit density and refractive index that are similar to those of the monomer and that the monomers do not interact, from the relation for φ_2/φ_1 in Ref. 46, we get

$$v_{aggregates} \approx \frac{\phi_2}{\phi_1} = \frac{A_2}{A_1}\left(\frac{R_1}{R_2}\right)^3 \quad (2)$$

where, the ratio $(R_1/R_2)^3$ stems from the Rayleigh's law, according to which the scattered intensity is proportional to the sixth power of the particle radius. We obtain that $v_{aggregates} \approx 0.001$. From the ratios φ_2/φ_1 and R_2/R_1, we compute the number concentration of large aggregates $n_{aggregates} \approx 10^{10}$ cm^{-3} Ref. 46. If the aggregation state of hematin in the red cells is similar to the one in the solution analyzed in Figure 2, with the volume of a red blood cell $\sim 90 \times 10^{-12}$ cm^3, there should be approximately one such aggregate per erythrocyte. Conversely, multiple, up to 10 HbS polymer often form in a single red blood cell, suggesting that the hematin aggregates seen in Figure 2 are unlikely factors for HbS polymer nucleation.

Further evidence against the participation of the heme aggregates in HbS polymerization comes from data on the effect of added hematin solution on the nucleation rate.[29] HbS nucleation kinetics was characterized in 260–280 mg ml^{-1} HbS solutions, which were shown to contain about 120–180 μM free heme.[29] The addition of 260 or 280 μM hematin, which increases the concentration of this reagent by at most 3.5×, led to 100× faster nucleation. The difference between these two numbers cannot be explained within the assumption of hematin aggregates serving as HbS polymer nucleation centers. Indeed, if the aggregate concentration in hematin solutions scales with the total hematin concentration, one would expect the increase in nucleation rate to be equal to the increase of hematin concentration, that is, at most 3.5×.

With this result, we explore the alternative hypothesis, that free heme accelerates the nucleation of HbS polymers using a thermodynamic mode of action. Below, we test if heme enhances the attraction between hemoglobin molecules, which, in turn, may stabilize nucleation precursors and accelerates HbS polymer nucleation.

Hematin Increases the Volume of the Nucleation Precursors

The two-step nucleation mechanism and the dense liquid clusters

Historically, it has been implicitly or explicitly assumed that the nucleation of sickle cell hemoglobin polymers is a one-step process: the disordered HbS molecules from the solution assemble into an ordered nucleus which has the same structure as long HbS fibers.[61,62] results indicated that this is not the case and HbS polymer nucleation follows a two-step mechanism,[46,63,64] that is, the formation of ordered polymer nuclei is preceded and occurs inside metastable dense liquid clusters, as illustrated in Figure 3.[65–70]

Metastable dense liquid clusters in deoxy-HbS solutions, within which the HbS polymer nucleation may occur, were characterized by dynamic light scattering.[46] Figure 4a shows a typical intensity correlation function of such solution. The correlation function reveals two processes: the one with

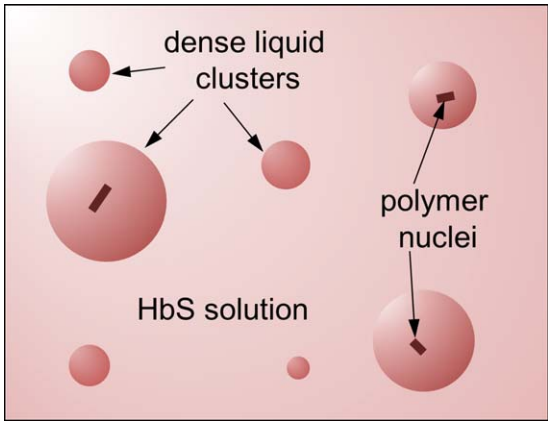

Figure 3. Schematic illustration of the two-step mechanism of nucleation of HbS polymer fibers.

Step 1 is the formation of dense liquid clusters. Step 2 is the formation of fiber nuclei within these droplets. [Color figure can be viewed in the online issue, which is available at wileyonlinelibrary.com.]

characteristic time of ~ 0.04 μs is the Brownian motion of single HbS molecules and it is present at all solution concentrations. A second process has a longer characteristic time and its amplitude increases with higher hemoglobin concentrations. It was shown that this slower time corresponds to HbS clusters suspended in the HbS solution, and not to single HbS molecules embedded in a loose network structure constraining their free diffusion.[46]

The mean hydrodynamic radius of the cluster population R_2 and the volume fraction ϕ_2 occupied by the clusters are determined from the correlation functions; several time-dependences of ϕ_2 are shown in Figure 4b.[46] From the data in Figure 4, the HbS clusters occupy $\phi_2 = 10^{-6} - 10^{-5}$ of the solution volume. Similar clusters of protein-rich liquid have been detected in solutions of several proteins: lumazine synthase,[71,72] lysozyme,[73,74] glucose isomerase,[75] and others, at electrolyte concentrations ranging from 20 mM[74] to 1.3 M,[71,72] by atomic force microscopy,[71] dynamic light scattering,[46,72–74] and UV resonance Raman spectroscopy.[76] With all studied proteins, the clusters are mesoscopic in size, from under one hundred to several hundred nanometers,[29,72,74] and liquid in nature.[72,77] The clusters occupy a low fraction of the solution volume: from $\sim 10^{-7}$ (below which they are not reliably detectable) to $\sim 10^{-3}$. The cluster volume fraction remains at these low levels even as the protein concentration in the bulk solution approaches that of the liquid within the clusters.[29,74] The mesoscopic clusters exist with similar characteristics both in the homogeneous region of the phase diagram of the protein solution (where no condensed phases, liquid or solid, are stable or present as long-lived metastable domains) and under conditions supersaturated with respect to ordered solid phases, such as crystals[72] or, as here, sickle cell hemoglobin polymers.[46,64] According to the two-step nucleation mechanism, in supersaturated solutions the clusters are crucial sites for the nucleation of ordered solid phases.[64,78,79] The protein clusters are similar to, but larger than clusters found in solutions of biominerals,[80–82] organic molecules,[83,84] polymers,[85] and colloids,[86–88] where they also play a crucial role in crystal nucleation.

The existence of mesoscopic clusters challenges our understanding of phases and phase equilibria.[74] Recent studies reveal that the small fraction of protein contained in the

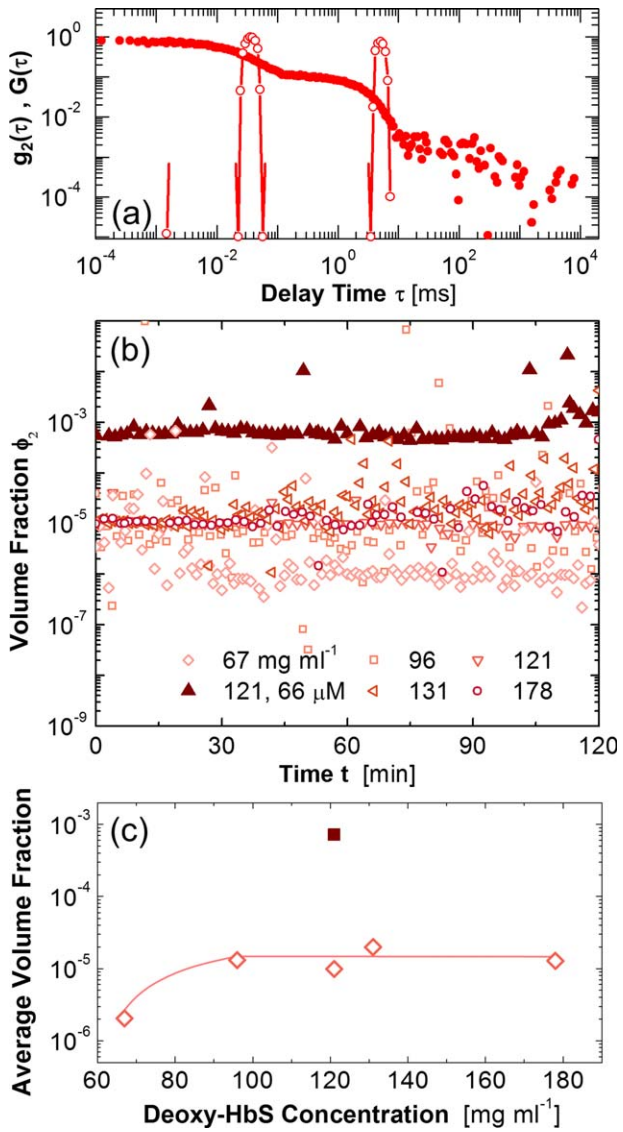

Figure 4. Light scattering characterization of dense liquid clusters.

(a) A correlation function (solid circles) and the respective delay time distribution function (open circles) of a deoxy-HbS solution with $C_{HbS} = 67$ mg ml^{-1}. (b) Time dependence of volume fraction ϕ_2 occupied by clusters, determined as in Ref. 46 at five HbS concentrations, shown in legend, and in the presence of shown concentration of heme at one of these HbS concentrations. (c) The dependence of the average volume fraction from (b) on HbS concentration. Solid symbol at 121 mg ml^{-1}: in the presence of 66 μM of free heme; open symbols: in the absence of heme. Line is just a guide for the eye. [Color figure can be viewed in the online issue, which is available at wileyonlinelibrary.com.]

clusters reflect the significant free energy cost of increasing the protein concentration.[74] The mesoscopic size of the clusters is significantly greater than the predictions of several mechanisms of cluster formation in protein and colloid solutions.[74,89] If these mechanisms are inactive, due to the free energy excess of high concentration protein liquid, the clusters should consist of just a few protein molecules, as indicated by a straightforward thermodynamic evaluation.[74] To solve the puzzle of the cluster size, we argued in Ref. 74 that the clusters largely consisted of transient protein complexes that formed at high protein concentrations. Several types of interactions: hydration, electrostatic, and the formation of domain-swapped dimers after partial protein misfolding, were considered and tested as possible bonds between the protein molecules in the transient complexes.[74]

Several of the predictions of the theory can be tested against the experimental observations of clusters in HbS solutions. The theory predicts that the cluster size is of order several hundred nanometers, and the clusters are composed of dense protein liquid: both of this predictions agree with the observations with HbS.[46]

Another prediction of the cluster theory in Ref. 74, which can be verified using the data in Figure 4 are that cluster formation is reversible and the clusters are in equilibrium with the solution. Correspondingly, the fraction of the hemoglobin in the clusters v_2 complies with the Boltzmann distribution and can be evaluated as $v_2 \approx \exp(-\Delta G(C_L,C_H)/k_BT)$, where $\Delta G(C_L,C_H)$ is the free energy excess of the dense liquid with concentration C_H over the HbS solution, with concentration C_L; $v_2 = C_H\varphi_2/(C_L\varphi_1 + C_H\varphi_2) \cong C_H\varphi_2/C_L\varphi_1$ is of the same order of magnitude, but somewhat higher as the ratio φ_2/φ_1.

To evaluate ΔG, we use the dependence of the KC/R_θ ratio on hemoglobin mass concentration C (K is a device constant, R_θ is the Raleigh ratio of the scattered to incident light[90]), determined by static light scattering[47,48] and displayed in Figure 5; for details about static light scattering in solutions which absorb the wavelength used in the determinations, see Ref. 74. This ratio is directly related to the inverse osmotic compressibility of the solution: $KC/R_\theta = (\partial\Pi/\partial C)/RT$ (Π is the contribution of the protein to the osmotic pressure, and R is the universal gas constant). We integrate the compressibility $\partial\Pi/\partial C$ it to compute the free energy $\Delta G = -\int_{C_L}^{C_H} \Pi dV + \Delta(\Pi V)$ needed to increase the concentration of N protein molecules from that in the dilute solution C_L to that in the dense liquid C_H. This allows us to determine ΔG as the free energy difference between states with concentrations C_L and C_H

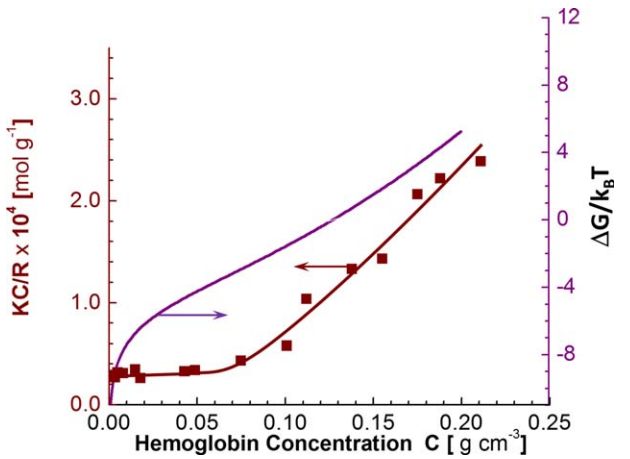

Figure 5. Right: The dependence of the ratio KC/R_θ on hemoglobin concentration C.

K: instrument constant, $R_\theta = I_\theta/I_0$– Raleigh ratio of intensities of scattered at angle $\theta = 90^\circ$ I_θ and incident light I_0, shown in brown. Left: Integration of data in (a) according to Eq. 1a to determine the solution free energy ΔG, shown in purple. [Color figure can be viewed in the online issue, which is available at wileyonlinelibrary.com.]

$$\frac{\Delta G(C_L, C_H)}{N k_B T} = \int_{C_L}^{C_H} \frac{d\rho}{C^2} \int_0^C M_w \left(\frac{KC'}{R_\theta}\right) dC' + \Delta \left[\frac{1}{C}\int_0^C M_w \left(\frac{KC'}{R_\theta}\right) dC'\right]_{C_L}^{C_H} \quad (3)$$

where, M_w is the molar mass of the protein.

The experimentally determined dependence $KC/R_\theta(C)$ in Figure 5 is fitted by a cubic polynomial and integrated using Eq. 3. The resulting$\Delta G/k_BT$, shown in Figure 5, varies between $-3.7\ k_BT$ at $C = 67$ mg ml^{-1} and $-1.5\ k_BT$ at $C = 96$ mg ml^{-1}. Thus, the free energy of the solution would increase by $2.2\ k_BT$ on this concentration increase. As the individual clusters are not affected by the concentration of the solution which generates them,[74] this increase would lead to a decrease of the excess free energy of the clusters above that of the solution. According to the Boltzmann distribution, the corresponding increase in cluster volume fraction would be about 9×, in agreement with the data in Figures 4b,c. The absorbance of hemoglobin of the wavelength used in the determinations of $KC/R_\theta(C)$ does not allow determinations at concentrations above 200 mg ml^{-1}. Hence, extrapolation to the suspected concentration in the clusters, ~400 mg ml^{-1}, would be unjustified and comparisons of the cluster volume fraction in Figures 4b,c to the predictions of the Boltzmann law are not feasible.

How does free heme affect HbS polymer nucleation?

Figures 4b,c show that the addition of free heme leads to increase in the cluster volume fraction ϕ_2 by about two orders of magnitude. The cluster radius is the same as in solutions without hematin, that is, the cluster number density also increases by two orders of magnitude. As the nuclei of HbS fibers form inside the metastable dense liquid clusters,[64,91] the faster J and shorter θ recorded in the presence of hematin directly correlate to the increase in ϕ_2. The factor of increase in the volume of the dense liquid clusters is equal to the factors of acceleration of HbS polymer nucleation and extension of the nucleation delay time. This correspondence renders powerful support for the action of the two-step nucleation mechanism in HbS polymer nucleation: as the clusters are the locations in which the polymers nucleate, this mechanism predicts that increasing their volume would lead to similar increase in the nucleation rate.

Thus, we have elucidated the first step in the mechanism of action of free heme. The next question is how does the free heme induce such increase in the cluster volume? To address this question, we use static light scattering to study interactions between protein molecules in solutions. The Kirkwood and Goldberg expression describing light scattering from multicomponent systems containing nonelectrolytes,[92,93] with assumptions that apply to HbS solutions,[47] becomes

$$\frac{KC}{\Delta R_\theta} = \frac{1}{M_{HbS}} + 2\alpha A_{12} C_{heme} + 2\left\{A_{22} + \left[\left(1 + 2\alpha \frac{M_{HbS}}{M_{heme}}\right) A_{212} - \frac{M_{HbS}}{2M_{heme}} A_{12}^2 + \alpha M_{HbS} A_{12} A_{22}\right] C_{heme}\right\} C \quad (4)$$

where $\Delta R_\theta = R_{\theta((1+2)} - R_{\theta 1} = (I_{\theta((1+2)} - I_{\theta 1})/I_0$: $R_{\theta((1+2)}$ and $I_{\theta((1+2)}$ are, respectively, the Rayleigh ratio and scattered intensity at angle θ for a solution containing both species and $R_{\theta 1}$ and $I_{\theta 1}$ are these variables in a the solution containing only free heme. A pair of subscripts of the virial coefficients A denotes that this coefficient relates to interactions between two molecules of the respective species. Thus, A_{22} characterizes interactions between two hemoglobin molecules; as the free heme concentration is low, its effects on these interactions are negligible and we assume $A_{22} \cong A_2$. A_{212} characterizes three-body interactions between two hemoglobin and one heme molecules. If the dependence $KC/\Delta R_\theta(C)$ is linear, according to Eq. 4, its intercept defines an apparent molecular mass $M_{HbS,app}$, and the slope—an effective second virial coefficient $A_{2,eff}$.

Both hemoglobin and free heme strongly absorb the illuminating wavelength and this absorption attenuates the intensity of the scattered light. It was shown that the errors in static and dynamic light scattering results due to absorption of light by the solution are minor.[94,95] The absorption modifies the Debye equation in a solution containing both hemoglobin and heme, but the absorption by these two molecules can be directly accounted for using the published values of their respective extinction coefficients at the wavelength of used for light scattering: for O_2-HbA $\varepsilon_2 = 0.561$ mM^{-1} cm^{-1}.[96] The extinction coefficient of heme at 632 nm, determined in our laboratory, is $\varepsilon_1 = 5.89$ mM^{-1} cm^{-1}.

To probe the effects of the heme on the intermolecular interactions, we first remove by dialysis any free heme that may have been released by the hemoglobin molecules. Heme at molar concentration $m_1 = 50\ \mu$M ($c_1 = 0.032$ mg ml^{-1}) was added to HbS solutions, whose concentration c_2 range corresponds to 80 μM $< m_2 <$ 300 μM. The Debye plots for deoxy-HbS are shown in the main plot of Figure 6, and those in the presence of added heme are shown in its inset. Form these Debye plots, we determine A_2 and M_2, or, in the case of heme-hemoglobin solutions, $A_{2,eff}$ and $M_{2,app}$. M_2 is compared with the known molecular mass of hemoglobin for a partial verification of the determinations, while $M_{2,app}$ is used to determine A_{12}, using Eq. 4 above. From $A_{2,eff}$, using A_{22}, A_{12}, we determine A_{212}.[47] These data show that $M_{HbS,app}$, and $A_{2,eff}$ decrease on the addition of heme. Straightforward thermodynamic analyses reveal that the decrease in $A_{2,eff}$ indicates that free heme enhances the attraction between the HbS molecules.

The enhanced attraction leads to slower increase of the chemical potential μ_2 of HbS as its concentration is increased. Quantification of this effect in Ref. 47 using an expression similar to Eq. 3 yields that the chemical potential of HbS in the clusters μ_2 is lowered by $\Delta\mu_2 = 4\ k_BT$ in the presence of 50 μM free heme from its value in a solution without free heme. A lower $\Delta\mu_2$ increases the cluster volume fraction by a factor of exp (4) = 50. This is consistent with the 80-fold increase of cluster volume fraction induced by 67 mM of free heme in Figures 4b,c.

An appropriate question at this point is how free heme concentrations as low as 50 μM significantly enhance the attraction between HbS molecules? The known biophysical mechanisms would require free heme concentrations significantly higher, or at least comparable to those of HbS. For instance, if heme were acting as a depletion or screening agent, m_{heme} would be orders of magnitude higher than m_{HbS}; if heme were forming bridges between HbS molecules, $m_{heme}/m_{HbS} \approx 1$.[97,98] We proposed a phenomenological model based on the osmotic virial coefficients in a three component solutions, A_{12} and A_{212}.[47] According to this model, repulsion by free heme prevents the hemoglobin

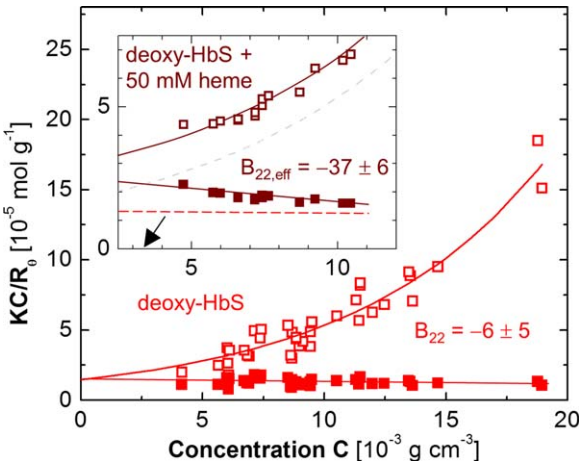

Figure 6. Characterization of the interactions between HbS molecules in deoxy-HbS solutions in terms of second virial coefficients B_{22}, extracted from Debye plots KC/R_θ (C).

K: instrument constant, $R_\theta = I_\theta/I_0$: ratio of scattered at angle θ to incident intensity, C: HbS concentration. Open symbols: measured I_θ is lowered because of absorption of light by HbS, line through points is a fit to a product of Debye and Beer equations: $KC/R_\theta \exp(-2.3\varepsilon Cl) = 1/M_w + 2A_{22}C$, where $\varepsilon = 4930.8$ cm^{-1} mol^{-1} l is the extinction coefficient of Hb at 628 nm, the wavelength used, $l = 0.8$ cm is the optical pathway in the cuvette, and M_w is the hemoglobin molecular weight. Solid symbols: I_θ is corrected with $\exp(-2.3\varepsilon Cl)$ and the data are fit with $KC/R_\theta = 1/M_w + 2A_{22}C$. The slope of this dependence is the second virial coefficient $A_{22} = -7.8 \times 10^{-5}$ mol cm^{-3} g^{-2}, nearly equal to a determination in Ref. 97. The dimensionless B_2, shown in plots, is determined from $A_{22} = B_{22}V_m M_w^{-2}$, where $V_m = 50560$ cm^3 mol^{-1} is the HbS molar volume. Values of $B_{22} < 4$, the value for noninteracting hard spheres, indicate intermolecular attraction. Main plot: Deoxy-HbS solution without the addition of free heme. At $C = 0$ g cm^{-3}, the data extrapolate to $1/M_w$, from which $M_w = 68\ 000 \pm 7{,}000$ g mol^{-1}, close to the actual 64,000 g mol^{-1}. Inset: 50 mM of heme added after dialysis. The additional absorption of light by free heme is accounted by calibrating against solution with same free heme concentration. The concentration of HbS at which the molar concentration of the HbS tetramer is equal to that of the added heme is marked with an arrow. Dashed lines indicate locations of data in the main plot. According to Eq. 4, the intercept of this straight line depends on the hemoglobin molecular mass M_w and on the virial coefficient A_{12} accounting for the interaction between free heme and hemoglobin. The dimensionless slope $B_{22,\mathrm{eff}}$ is more negative than B_{22} in solutions without free heme in the main plot. This indicates stronger effective attraction between the hemoglobin molecules in the presence of free heme. [Color figure can be viewed in the online issue, which is available at wileyonlinelibrary.com.]

molecules from accessing parts of the volume; this acts as effective attraction. Indeed, the Debye length $k^{-1} \approx 1$ nm at the ionic strength $I \approx 150$ mM of the phosphate buffer used here. Assuming that electrostatic repulsion lowers the probability of finding a hemoglobin molecule within 10 such lengths, the volume excluded by one heme molecule is ca. 1500 nm^3. The fraction of the solution volume excluded by 50 μM of heme would be 0.05, a significant number. The heme effects on HbS intermolecular attraction may be additionally enhanced by the high mobility of heme: its effective hydrodynamic radius is ca. 0.2 that of hemoglobin.

Conclusions

We have shown that the concentration of free heme in the cytosol of sickle and healthy erythrocytes is significant: 44 and 21 μM, respectively. These concentrations are comparable to the concentrations found to lead to a significant acceleration of sickle cell hemoglobin polymerization. Thus, free heme may be an important factor for faster HbS polymerization and the variability in free heme concentration may contribute to the mysterious variability and unpredictability of the disease.

Exploring the mechanism of action of free heme, we have shown that a kinetic mechanism, whereby heme aggregates serve as heterogeneous centers for faster HbS polymer nucleation does not apply. We have demonstrated a purely thermodynamic mechanism: free heme in HbS solutions enhances the attraction between hemoglobin molecules. The stronger attraction leads to greater volume fraction of the metastable dense liquid clusters, which, in turn, leads to faster nucleation of the sickle cell hemoglobin polymers. We have demonstrated a quantitative correlation between the hemoglobin chemical potential change due to the enhanced attraction, the increase in the volume occupied by the nucleation precursors, and the acceleration of polymer nucleation in the presence of free heme.

As the experiment conditions mimic those inside the red cell cytosol it is likely that hematin released from hemoglobin in the red cells would have similar effects on the nucleation of sickle cell polymers *in vivo*. The concentration of free hematin in the red cells is lowered by three processes: diffusion thorough the cell membrane,[100] association to the membrane or the cytoskeleton,[101] or intracellular degradation.[102] Their combined action could lead to significant variability of the hematin concentration in the red cells. Because of the high sensitivity of the rates of nucleation and growth of sickle cell polymers to hematin concentration, this variability could lead to significant irreproducibility of polymerization between the red cells of identical HbS activities of a patient. The variability of hematin release and removal between patients could be the factor underlying the variability in the prognosis of patients with identical HbS expression. A more significant conclusion from our results is that if the free hematin concentration in the erythrocytes is lowered, this could result in lower sickling and less severe sickle cell symptoms.

Conversely, a correlation should be present between free heme concentration and clinical outcomes. For instance if the level of methemoglobin is strongly correlated with the concentration of free heme in the red cells, then the level of methemoglobinemia (high methemoglobin content) would correlate with disease severity. The studies of the effects of methemoglobinemia in literature focused on severe cases, where the concentration of met-hemoglobin is up to 20% of the total.[103] They found that due to the significant decrease in HbS activity, such high methemoglobin concentrations ameliorate the disease. To test the implications of free heme for patient outcomes, patients with methemoglobin concentrations of several percent should be recruited. If free heme concentration corresponds to higher methemoglobinemia, the methemoglobin amount should correlate with the disease severity.

If the variation in heme concentration explains the mysterious clinical variability among patients with similar HbS concentration, it may also explain the vast clinical difference

between hemoglobin SC disease (patients are heterozygous for hemoglobins C and S) and sickle trait, where the HbS concentrations are similar, but the clinical courses are wildly different. The same is true for sickle-beta-zero thalassemia, where the HbS concentration is significantly lower than in homozygous SS, but the clinical outcomes are often similar. Measurements of free heme for these patients would be informative.

Last, it is possible that the hematin released in infected red blood cells by malaria plasmodia as a byproduct of their metabolism of hemoglobin[104] causes the known sickling of sickle-trait erythrocytes (which would not sickle in the absence of hematin because of lower HbS activity) and enables their selective removal from the circulation.[105] This may be a novel explanation of the link between malaria and sickle cell disease.

Acknowledgments

The authors are deeply indebted to R.C. Willson for help with the procedure for free heme determination and for generous access to the Tecan Microplate Reader, K. Waller, RN, and J. Nguyen, RN, from the UH Health Center for competent and expeditious assistance in the collection of blood from healthy donors, A. Linsey and R. Fuller from the Gulf Coast Regional Blood Center for sickle trait and healthy blood samples, and B. Dinu and G. Airewele from Texas Children's Hospital for sickle cell blood. This work was supported by NIH (Grant U01HL114476), the Norman Hackerman Advanced Research Program (Grant 003652-0078-2009), and NSF (Grant MCB-1244568).

Literature Cited

1. Pauling L, Itano HA, Singer SJ, Wells IC. Sickle cell anemia, a molecular disease. *Science*. 1949;111:543–548.
2. Eaton WA. Linus Pauling and sickle cell disease. *Biophys Chem.* 2003;100(1–3):109–116.
3. Ingram VM. A specific chemical difference between the globins of normal human and sickle cell anaemia haemoglobin. *Nature*. 1956; 178:792–794.
4. Dykes GW, Crepeay RH, Edelstein SJ. Three dimensional reconstruction of the fibers of sickle cell haemoglobin. *Nature*. 1978;272: 506–510.
5. Dykes GW, Crepeay RH, Edelstein SJ. Three dimensional reconstruction of 14-filament fibers of hemoglobin S. *J Mol Biol*. 1979; 130:451–472.
6. Carrager B, Bluemke DA, Gabriel B, Potel MJ, Josephs R. Structural analysis of polymers of sickle cell hemoglobin. *I. Sickle cell hemoglobin fibers. J Mol Biol*. 1988;199(2):315–331.
7. Nelson DL, Cox MM. *Lehninger's Principles of Biochemistry*, 3rd ed. New York: W.H. Freeman, 2000.
8. Wishner B, Ward K, Lattman E, Love W. Crystal structure of sickle-cell deoxyhemoglobin at 5 A resolution. *J Mol Biol*. 1975;98: 179–194.
9. Fronticelli C, Gold R. Conformational relevance of the beta6Glu replaced by Val mutation in the beta subunits and in the beta(1–55) and beta(1–30) peptides of hemoglobin S. *J Biol Chem*. 1976; 251(16):4968–4972.
10. Mickols W, Maestre MF, Tinoco I Jr, Embury SH. Visualization of oriented hemoglobin S in individual erythrocytes by differential extinction of polarized light. *Proc Natl Acad Sci USA*. 1985;82(19): 6527–6531.
11. Briehl RW. Rheology of hemoglobin S gels: possible correlation with impaired microvascular circulation. *Am J Pediatr Hematol Oncol*. 1983;5:390–398.
12. Samuel RE, Salmon ED, Briehl RW. Nucleation and growth of fibres and gel formation in sickle cell haemoglobin. *Nature*. 1990; 345:833–835.
13. Higgins JM, Eddington DT, Bhatia SN, Mahadevan L. Sickle cell vasoocclusion and rescue in a microfluidic device. *Proc Natl Acad Sci USA*. 2007 ;104(51):20496–20500.
14. Beutler E. The sickle cell diseases and related disorders. In: Beutler E, Lichtman MA, Coller BS, Kipps TJ, Seligsohn U, editors. *Williams Hematology*, 6th ed. New York: McGraw Hill;2001:581–605.
15. Bunn HF, Jandl JH. Exchange of heme among hemoglobins and between hemoglobin and albumin. *J Biol Chem*. 1968;243(3):465–475.
16. Hargrove MS, Whitaker T, Olson JS, Vali RJ, Mathews AJ. Quaternary structure regulates hemin dissociation from human hemoglobin. *J Biol Chem*.1997;272(28):17385–17389.
17. Hebbel RP, Morgan WT, Eaton JW, Hedlund BE. Accelerated autoxidation and heme loss due to instability of sickle hemoglobin. *Proc Natl Acad Sci USA*. 1988;85(1):237–241.
18. Kirschner-Zilber I, Rabizadeh E, Shaklai N. The interaction of hemin and bilirubin with the human red cell membrane. *Biochim BiophysActa*. 1982;690(1):20–30.
19. Fitch C, Chevli R, Kanjananggulpan P, Dutta P, Chevli K, Chou A. Intracellular ferriprotoporphyrin IX is a lytic agent. *Blood*. 1983 ; 62(6):1165–1168.
20. Goldstein L, Teng ZP, Zeserson E, Patel M, Regan RF. Hemin induces an iron-dependent, oxidative injury to human neuron-like cells. *J Neurosci Res*. 2003;73(1):113–121.
21. Kuross SA, Rank BH, Hebbel RP. Excess heme in sickle erythrocyte inside-out membranes: possible role in thiol oxidation. *Blood*. 1988; 71(4):876–882.
22. Wagener FADTG, Abraham NG, van Kooyk Y, de Witte T, Figdor CG. Heme-induced cell adhesion in the pathogenesis of sickle-cell disease and inflammation. *Trends Pharmacol Sci*. 2001;22(2):52–54.
23. Amin BR, Bauersachs RM, Meiselman HJ, Mohandas N, Hebbel RP, Bowen PE, Schlegel RA, Williamson P, Westerman MP. Monozygotic twins with sickle cell anemia and discordant clinical courses: clinical and laboratory studies. *Hemoglobin*. 1991;15(4):247–256.
24. Adisa OA, Hu Y, Ghosh S, Aryee D, Osunkwo I, Ofori-Acquah SF. Association between plasma free haem and incidence of vaso-occlusive episodes and acute chest syndrome in children with sickle cell disease. *Br J Haematol*. 2013;162(5):702–705.
25. Nabel EG, Shurin SB. A recommitment to sickle cell disease research. *Blood*. 2008;111(10):4852–4853.
26. Embury SH. The not-so-simple process of sickle cell vasoocclusion. *Microcirculation*. 2004;11:101–113.
27. Hebbel RP. Special issue of microcirculation: examination of the vascular pathobiology of sickle cell anemia. *Microcirculation*.;11(2): 99–100.
28. Hebbel RP, Osarogiagbon R, Kaul D. The endothelial biology of sickle cell disease: inflammation and a chronic vasculopathy. *Microcirculation*. 2004;11(2):129–151.
29. Uzunova VV, Pan W, Galkin O, Vekilov PG. Free heme and the polymerization of sickle cell hemoglobin. *Biophys J*. 2010;99(6): 1976–1985.
30. Liu SC, Zhai S, Palek J. Detection of hemin release during hemoglobin S denaturation. *Blood*. 1988;71(6):1755–1758.
31. de Villiers KA, Kaschula CH, Egan TJ, Marques HM. Speciation and structure of ferriprotoporphyrin IX in aqueous solution: spectroscopic and diffusion measurements demonstrate dimerization, but not mu-oxo dimer formation. *J Biol Inorg Chem*.2007;12(1):101–117.
32. Asher C, de Villiers KA, Egan TJ. Speciation of ferriprotoporphyrin IX in aqueous and mixed aqueous solution is controlled by solvent identity, pH, and salt concentration. *Inorg Chem*. 2009;48(16):7994–8003.
33. Kashchiev D. *Nucleation. Basic Theory with Applications*. Oxford: Butterworth, Heinemann, 2000.
34. Prausnitz J, Foose L. Three frontiers in the thermodynamics of protein solutions. *Pure Appl Chem*. 2007;79(8):1435–1444.
35. Prausnitz JM. Molecular thermodynamics for some applications in biotechnology. *J Chem Thermodyn*. 2003;35:21–39.
36. Neugebauer U, Marz A, Henkel T, Schmitt M, Popp J. Spectroscopic detection and quantification of heme and heme degradation products. *Anal Bioanal Chem* 2012;404(10):2819–2829.
37. Luo D, Huang J. Determination of cytochrome c and other heme proteins using the reduction wave of mercury protoporphyrin IX groups generated by a hydroxylamine induced replacement reaction. *Anal Chem*. 2009;81(5):2032–2036.
38. Appaix F, Minatchy M-N, Riva-Lavieille C, Olivares J, Antonsson B, Saks VA. Rapid spectrophotometric method for quantitation of

cytochrome c release from isolated mitochondria or permeabilized cells revisited. *Biochimica Biophy Acta*. 2000;1457(3):175–181.
39. Crouser ED, Gadd ME, Julian MW, Huff JE, Broekemeier KM, Robbins KA, Pfeiffer DR. Quantitation of cytochrome c release from rat liver mitochondria. *Anal Biochem*. 2003;317(1):67–75.
40. Tan SN, Hua L. Amperometric detection of cytochrome c by capillary electrophoresis at a sol–gel carbon composite electrode. *Anal Chim Acta*. 2001;450(1–2):263–267.
41. Scheller FW, Bistolas N, Liu S, Jänchen M, Katterle M, Wollenberger U. Thirty years of haemoglobin electrochemistry. *Adv Colloid Interface Sci*. 2005;116(1–3):111–120.
42. Whiteaker JR, Fenselau CC, Fetterolf D, Steele D, Wilson D. Quantitative determination of heme for Forensic characterization of Bacillus spores using matrix-assisted laser desorption/ionization time-of-flight mass spectrometry. *Anal Chem*. 2004;76(10):2836–2841.
43. Takahashi S, Masuda T. High throughput heme assay by detection of chemiluminescence of reconstituted horseradish peroxidase. *Comb Chem High Throughput Screen*. 2009;12(5):532–535.
44. Huntress E, Stanley L, Parker A. The preparation of 3-Aminophthalhydrazide for use in the demonstration of chemiluminescence. *J Am Chem Soc*. 1934;56(1):241–242.
45. Huntress EH, Stanley LN, Parker AS. The oxidation of 3-aminophthalhydrazide ("luminol") as a lecture demonstration of chemiluminescence. *J Chem Educ*. 1934;11(3):142.
46. Pan W, Galkin O, Filobelo L, Nagel RL, Vekilov PG. Metastable mesoscopic clusters in solutions of sickle cell hemoglobin. *Biophys J*. 2007;92(1):267–277.
47. Pan W, Uzunova VV, Vekilov PG. Free heme in micromolar amounts enhances the attraction between sickle cell hemoglobin molecules. *Biopolymers*. 2009;91(12):1108–1116.
48. Vekilov PG, Feeling-Taylor AR, Petsev DN, Galkin O, Nagel RL, Hirsch RE. Intermolecular interactions, nucleation and thermodynamics of crystallization of hemoglobin C. *Biophys J*. 2002;83:1147–1156.
49. Gibbs JW. On the equilibrium of heterogeneous substances, First Part. *Trans Connect Acad Sci*. 1876;3:108–248.
50. Gibbs JW. On the equilibrium of heterogeneous substances (concluded). *Trans Connect Acad Sci*. 1878;3:343–524.
51. Gibbs JW. *The Scientific Papers of J.W. Gibbs. Volume One Thermodynamics*. Woodbridge, Connecticut: Oxbow Press, 1993.
52. Kertis F, Khurshid S, Okman O, Kysar JW, Govada L, Chayen N, Erlebacher J. Heterogeneous nucleation of protein crystals using nanoporous gold nucleants. *J Mater Chem*. 2012.
53. Chayen NE, Saridakis E, Sear RP. Experiment and theory for heterogeneous nucleation of protein crystals in a porous medium. *Proc Natl Acad Sci USA*. 2006;103(3):597–601.
54. Page AJ, Sear RP. Heterogeneous nucleation in and out of Pores. *Phys Rev Lett*. 2006;97(6):065701.
55. Diao Y, Harada T, Myerson AS, Hatton TA, Trout BL. The role of nanopore shape in surface-induced crystallization. *Nat Mater*. 2011;10(11):867–871.
56. Quillin ML, Matthews BW. Accurate calculation of the density of proteins. *Acta Crystallogr D Biol Crystallogr*. 2000;56(7):791–794.
57. MA, Olafson KN, Petrova EV, Rimer JD, Vekilov PG. Hematin crystallization from aqueous and organic solvents. *J Chem Phys*. 2013;139(12):121911.
58. Egan TJ. Recent advances in understanding the mechanism of hemozoin (malaria pigment) formation. *J Inorg Biochem*. 2008;102(5–6):1288–1299.
59. Olafson KN, Rimer JD, Vekilov PG. Growth of large hematin crystals in biomimetic solutions. *Cryst Growth Des*. 2014;14(5):2123–2127.
60. Li Y, Lubchenko V, Vorontsova MA, Filobelo L, Vekilov PG. Ostwald-like ripening of the anomalous mesoscopic clusters in protein solutions. *J Phys Chem B*. 2012;116(35):10657–10664.
61. Ferrone FA, Hofrichter H, Eaton WA. Kinetics of sickle cell hemoglobin polymerization I. Studies using temperature jump and laser photolysis techniques. *J Mol Biol*. 1985;183:591–610.
62. Ferrone FA, Hofrichter H, Eaton WA. Kinetics of sickle cell hemoglobin polymerization. II. A double nucleation mechanism. *J Mol Biol*. 1985;183:611–631.
63. Galkin O, Nagel RL, Vekilov PG. The kinetics of nucleation and growth of sickle cell hemoglobin fibers. *J Mol Biol*. 2007;365(2):425–439.
64. Galkin O, Pan W, Filobelo L, Hirsch RE, Nagel RL, Vekilov PG. Two-step mechanism of homogeneous nucleation of sickle cell hemoglobin polymers. *Biophys J*. 2007;93:902–913.
65. Galkin O, Vekilov PG. Control of protein crystal nucleation around the metastable liquid-liquid phase boundary. *Proc Natl Acad Sci USA*. 2000;97(12):6277–6281.
66. Anderson VJ, Lekkerkerker HNW. Insights into phase transition kinetics from colloid science. *Nature*. 2002;416:811–815.
67. ten Wolde PR, Frenkel D. Enhancement of protein crystal nucleation by critical density fluctuations. *Science*. 1997;277:1975–1978.
68. Vekilov PG. Dense liquid precursor for the nucleation of ordered solid phases from solution. *Cryst Growth Des*. 2004;4:671–685.
69. Lutsko JF, Nicolis G. Theoretical evidence for a dense fluid precursor to crystallization. *Phys Rev Lett*. 2006;96:046102.
70. Shiryayev A, Gunton JD. Crystal nucleation for a model of globular proteins. *J Chem Phys*. 2004;120(17):8318–8326.
71. Gliko O, Neumaier N, Pan W, Haase I, Fischer M, Bacher A, Weinkauf S, Vekilov PG. A metastable prerequisite for the growth of lumazine synthase crystals. *J Am Chem Soc*. 2005;127:3433–3438.
72. Gliko O, Pan W, Katsonis P, Neumaier N, Galkin O, Weinkauf S, Vekilov PG. Metastable liquid clusters in super- and undersaturated protein solutions. *J Phys Chem B*. 2007;111(12):3106–3114.
73. Georgalis Y, Umbach P, Saenger W, Ihmels B, Soumpasis DM. Ordering of fractal clusters in crystallizing lysozyme solutions. *J Am Chem Soc*. 1999;121(8):1627–1635.
74. Pan W, Vekilov PG, Lubchenko V. The origin of anomalous mesoscopic phases in protein solutions. *J Phys Chem B*. 2010;114:7620–7630.
75. Sleutel M, Van Driessche AE. Role of clusters in nonclassical nucleation and growth of protein crystals. *Proc Natl Acad Sci USA*. 2014;111(5):E546–553.
76. Knee KM, Mukerji I. Real time monitoring of sickle cell hemoglobin fiber formation by UV resonance Raman spectroscopy. *Biochemistry*.2009;48(41):9903–9911.
77. Vekilov PG, Pan W, Gliko O, Katsonis P, Galkin O. Metastable mesoscopic phases in concentrated protein solutions. In: Franzese G, Rubi M, editors. *Lecture Notes in Physics, vol*. 752: *Aspects of Physical Biology: Biological Water, Protein Solutions, Transport and Replication*. Heidelberg: Springer, 2008:65–95.
78. Vekilov PG. Nucleation. *Cryst Growth Des*. 2010;10(12):5007–5019.
79. Brubaker WD, Freites JA, Golchert KJ, Shapiro RA, Morikis V, Tobias DJ, Martin RW. Separating instability from aggregation propensity in [gamma]S-crystallin variants. *Biophys J*. 2011;100(2):498–506.
80. Pouget EM, Bomans PHH, Goos JACM, Frederik PM, de With G, Sommerdijk NAJM. The initial stages of template-controlled CaCO3 formation revealed by cryo-TEM. *Science*. 2009;323(5920):1455–1458.
81. Gebauer D, Volkel A, Colfen H. Stable Prenucleation calcium carbonate clusters. *Science*. 2008;322(5909):1819–1822.
82. Gower LB. Biomimetic model systems for investigating the amorphous precursor pathway and its role in biomineralization. *Chem Rev*. 2008;108(11):4551–4627.
83. Erdemir D, Lee AY, Myerson AS. Nucleation of crystals from solution: classical and two-step models. *Acc Chem Res*. 2009;42(5):621–629.
84. Aber JE, Arnold S, Garetz BA. Strong dc electric field applied to supersaturated aqueous glycine solution induces nucleation of the polymorph. *Phys Rev Lett*. 2005;94:145503.
85. Wang JF, Muller M, Wang ZG. Nucleation in A/B/AB blends: Interplay between microphase assembly and macrophase separation. *J Chem Phys*. 2009;130(15):154902.
86. Leunissen ME, Christova CG, Hynninen A-P, Royall CP, Campbell AI, Imhof A, Dijkstra M, van Roij R, van Blaaderen A. Ionic colloidal crystals of oppositely charged particles. *Nature*. 2005;437(7056):235–240.
87. Savage JR, Dinsmore AD. Experimental evidence for two-step nucleation in colloidal crystallization. *Phys Rev Lett*. 2009;102(19):198302.
88. Zhang TH, Liu XY. Multistep crystal nucleation: a kinetic study based on colloidal crystallization. *J Phys Chem B*. 2007;111(50):14001–14005.
89. Hutchens SB, Wang Z-G. Metastable cluster intermediates in the condensation of charged macromolecule solutions. *J Chem Phys*. 2007;127:084912.
90. Schmitz KS. *Dynamic Light Scattering by Macromolecules*. New York: Academic Press, 1990.

91. Galkin O, Chen K, Nagel RL, Hirsch RE, Vekilov PG. Liquid-liquid separation in solutions of normal and sickle cell hemoglobin. *Proc Natl Acad Sci USA*. 2002;99:8479–8483.
92. Kirkwood JG, Goldberg RJ. Light scattering arising from composition fluctuations in multi-component systems. *J Chem Phys*. 1950; 18(1):54–57.
93. Bloustine J, Virmani T, Thurston GM, Fraden S. Light scattering and phase behavior of lysozyme-poly(ethylene glycol) mixtures. *Phys Rev Lett*. 2006;96(8):087803.
94. Sehgal A, Seery TAP. Anomalous dynamic light scattering from solutions of light absorbing polymers. *Macromolecules*. 1999;32:7807–7814.
95. Hall RS, Oh YS, Johnson CS Jr. Photon correlation spectroscopy in strongly absorbing and concentrated samples with applications to unliganded hemoglobln. *J Phys Chem*. 1980;84:756–767.
96. Prahl S. *Optical Absorption of Hemoglobin*. Available at: http://omlc.org/spectra/hemoglobin/. Accessed 2 April 2015.
97. Elbaum D, Nagel RL, Brookchin RM, Herskovits TT. Effects of alkylureates on the polymerization of hemoglobin S. *Proc Natl Acad Sci USA*. 1974;71:4718–4722.
98. Leckband D, Israelachvili J. Intermolecular forces in biology. *Q Rev Biophysics*. 2001;34:105–267.
99. Israelachvili JN. *Intermolecular and Surface Forces*. New York: Academic Press, 1995.
100. Cannon JB, Kuo, F., Pasternack, R. F., Wong, N. M., Muller-Eberhard, U. Kinetics of the interaction of hemin liposomes with heme binding proteins. *Biochemistry*. 1984;23:3715–3721.
101. Rank BH, Carlsson J, Hebbel RP. Abnormal redox status of membrane-protein thiols in sickle erythrocytes. *J Clin Invest*. 1985; 75(5):1531–1537.
102. Atamna H, Ginsburg H. Heme degradation in the presence of glutathione. A proposed mechanism to account for the high levels of non-heme iron found in the membranes of hemoglobinopathic red blood cells. *J Biol Chem*. 1995;270(42):24876–24883.
103. Beutler E. The effect of methemoglobin formation in sickle cell disease. *J Clin Invest*. 1961;40:1856–1871.
104. Jani D, Nagarkatti R, Beatty W, Angel R, Slebodnick C, Andersen J, Kumar S, Rathore D. HDP– A novel heme detoxification protein from the malaria parasite. *PLoS Pathogens*. 2008;4(4):e1000053.
105. Nagel RL. Malaria and hemoglobinopathies. In: Steinberg MH, Forget BG, Higgs DR, Nagel RL, editors. *Disorders of hemoglobin: Genetics, Pathophysiology and Clinical Management*. Cambridge: Cambridge University, 2001:832–860.

Manuscript received Jan. 5, 2015, and revision received Feb. 13, 2015.